The Journal of Engineering

The 7th International Conference on Renewable Power Generation (RPG 2018)

IET Journals
The Institution of Engineering and Technology

Voltage stability index and APFC for performance improvement of modern power systems with intense renewables

eISSN 2051-3305
Received on 22nd November 2018
Accepted on 10th January 2019
doi: 10.1049/joe.2018.9375
www.ietdl.org

Pradeep Singh[1] ✉, Rajive Tiwari[1], Mukesh Kumar Shah[1], Khaleequr Rahman Niazi[1], Nand Kishor Meena[2], Saurabh Ratra[1]

[1]*Department of Electrical Engineering, Malaviya National Institute of Technology, Jaipur, India*
[2]*Department of Electrical Engineering, Government Women Engineering College, Ajmer, India*
✉ *E-mail: psn121988@gmail.com*

Abstract: In this study, a newly developed amalgam power flow controller (APFC) is used for better controllability and voltage stability enhancement of modern power system with deep renewable penetration. A new voltage stability index is proposed to determine the potential site of APFC and then Grey Wolf optimisation based on fuzzy logic is adopted to determine the optimal parameter settings of the APFC. A quarter cosine and exponential fuzzy membership function have been used to find out membership value of diverse objectives. The multi-objective problem is formulated considering three different objectives of conflicting nature. The proposed optimisation framework is implemented on an IEEE benchmark system of 30 buses for different cases. The comparison of simulation results reveals the effectiveness of the proposed model.

1 Introduction

Nowadays, the electrical power system is experiencing new challenges due to various technical, economical and environmental constraints, which has led to stressed operating conditions. The stressed operating conditions may lead the system to voltage instability and loss of economy if corrective control actions are not taken [1]. Numerous incidents associated to voltage instability have been reported globally [1, 2]. The insufficient reactive power, heavy loading on the transmission line and power shipping across long distances play a vital role in consequent blackouts and voltage collapse. The flexible AC transmission system (FACTS) devices have been utilised to the adequate operation of existing system infrastructures by controlling the power flow over designated transmission routes. FACTS devices are also used to enhance voltage stability margin and system security. As the FACTS devices control the power flow in transmission lines, the system losses can be reduced, i.e. the efficiency of the system can be improved [3–5]. Each device has its own advantages and limitations, and zone of application. In this paper, a newly developed amalgam power flow controller (APFC) FACTS device is selected as it is more superior among all the FACTS devices available in the literature [6]. As suggested in [7], the most effective use of FACTS devices depends on the location and optimal parameter setting of these devices. Therefore, the proper placement of the FACTS devices is very crucial to extract maximum possible benefits.

In the literature, various techniques have been used to optimally allocate FACTS devices in a transmission system which can be classified into three broad categories: classical optimisation methods, evolutionary computation techniques and index-based methods. Index-based methods such as sensitivity index [8], extended voltage phasors approach [9], bus participation factor [10] and residue method [11] identify the weak nodes in the system. The placement of FACTS devices at these locations benefits in terms of increased voltage stability margin, reduced losses and optimised loading of transmission network [3–5]. Generally, analytical methods sometimes fail to determine optimal parameter setting in an efficient manner and also suffer from slow convergence. On the other hand, metaheuristics methods can determine the optimal solution of complex optimisation problems. Some well-established algorithms such as genetic algorithm [12], particle swarm optimisation [3], sparse optimisation [13] and self-adaptive fire-fly algorithm [14] have been used for FACTS devices allocation. As per the author's knowledge, the optimal location and their parameters setting of APFC has not been investigated. The FACTS devices placement and parameter setting problem is a multi-objective (MO) optimisation problem. Fuzzy logic due to its nature has shown potential to transform multiple-objectives into a single-objective function. Fuzzy framework [15, 16] offers a means to combine the objectives which are conflicting and also ensures a minimum degree of satisfaction among the different objectives.

This paper proposes a new voltage stability index for recognising the most sensitive node to voltage collapse in the network. The index is based on the area under the PV curve for determining weak nodes in the transmission system. Furthermore, the index is used to allocate the APFC optimally. The Grey Wolf optimisation (GWO) algorithm based on fuzzy logic-based approach is proposed to find the optimal parameter setting of APFC in the presence and absence of wind farms.

2 Proposed voltage stability index formulation

Let us consider the N bus system, where G and L denote the generator and load buses, respectively. By applying the nodal analysis, the following nodes current injection equation can be obtained:

$$[I_G] = [Y_{GG}][V_G] + [Y_{GL}][V_L] \tag{1}$$

$$[-I_L] = [Y_{LG}][V_G] + [Y_{LL}][V_L] \tag{2}$$

By putting the value of $[V_G]$ from (1) to (2), we obtain

$$[V_L] = [W_{LL}]^{-1}[I_L] + [W_{LL}]^{-1}[Y_{LG}][Y_{GG}]^{-1}[I_G] \tag{3}$$

where $[W_{LL}] = [Y_{LG}][Y_{GG}]^{-1}[Y_{GL}] - [Y_{LL}]$. Pre- and post-multiplying (3) by $[Y_{LL}]$ and $[Y_{LL}]^{-1}$, the following equation can be obtained:

$$[V_L] = [Y_{LL}]^{-1}[I_{eq(L)}] + [V_{eq(G)}] \tag{4}$$

where $[I_{eq(L)}] = [Y_{LL}][W_{LL}]^{-1}[I_L]$ and $[V_{eq(G)}] = [W_{LL}]^{-1}[Y_{LG}][Y_{GG}]^{-1}[I_G]$. Equation (4) can be viewed as

the voltage equation for the equivalent two-bus system as shown in Fig. 1. Therefore, for any load bus k, (4) can be interpreted as follows:

$$\frac{V_k}{V_{\mathrm{eq}(g)}} = 1 + \frac{I_{\mathrm{eq}(k)}}{Y_{kk}} \tag{5}$$

As $S_{\mathrm{eq}(k)} = V_k I^*_{\mathrm{eq}(k)}$, (5) can be expressed as

$$\frac{V_k}{V_{\mathrm{eq}(g)}} = 1 + \frac{S^*_{\mathrm{eq}(k)} V^*_{\mathrm{eq}(g)}}{Y_{kk} V^*_k V_{\mathrm{eq}(g)} V^*_{\mathrm{eq}(g)}} \tag{6}$$

By rearranging (6), we obtain

$$\left|\frac{V_k}{V_{\mathrm{eq}(g)}}\right|^2 - \frac{V^*_k}{V^*_{\mathrm{eq}(g)}} = \frac{S^*_{\mathrm{eq}(k)}}{Y_{kk}\left|V_{\mathrm{eq}(g)}\right|^2} \tag{7}$$

Assume $x = V_k/V_{\mathrm{eq}(g)}$, $\phi = \tan^{-1}[\Im(x)/\Re(x)]$ and $\alpha + \mathrm{j}\beta = S^*_{\mathrm{eq}(k)}/(Y_{kk}|V_{\mathrm{eq}(g)}|^2)$. Now, separate (7) into real and imaginary parts as follows:

$$|x|^2 - |x|\cos\phi = \alpha \tag{8}$$

$$|x|\sin\phi = \beta \tag{9}$$

By adding (8) and (9), we obtain

$$|x|^2 + (\sin\phi - \cos\phi)|x| - (\alpha + \beta) = 0 \tag{10}$$

Equation (10) is a quadratic equation. The graphical representation of this equation is shown in Fig. 2. The roots of (10) can be expressed as follows:

$$r_1,\ r_2 = \frac{\cos\phi - \sin\phi \pm \sqrt{(\cos\phi - \sin\phi)^2 + 4(\alpha + \beta)}}{2} \tag{11}$$

If r_1 and r_2 are the roots of the quadratic equation, then the area under the curve can be expressed as follows:

$$A = \int_{r_1}^{r_2} f(|x|)d|x| \tag{12}$$

Therefore, the proposed area-based voltage stability index (AVSI) can be expressed as

$$\mathrm{AVSI} = \frac{A}{2 \times A_0} \tag{13}$$

where A_0 is the area under the curve at the no-load condition and it can be calculated from (10) by assuming $S_{\mathrm{eq}k}$ is equal to zero. It is used to make AVSI equal to unity at the no-load condition. As the system moves toward the saddle-node bifurcation point, the area enclosed by curve decreases. Therefore, the proposed index, AVSI varies from unity (no-load) to zero (voltage collapse). On the other hand, all the buses can be ranked using the proposed index as the proposed index moves toward zero as the system move toward its stability limits. Mathematically, the most critical bus can be identified as

$$\min_k \ \mathrm{AVSI};\ k \in L \tag{14}$$

3 Amalgam power flow controller

A newly developed flexible, reliable and cost-effective APFC [6] FACTS device shown in Fig. 3 is used. The APFC is composed of the large capacity of SEN transformer and small rating distributed power flow controller to overcome the limitations of other FACTS devices. In APFC, the real power is mainly exchanged through the SEN transformer and to maintain the voltage of capacitors, the real power is also transferred through the transmission line at the third-harmonic frequency. To provide a return path for third-harmonic frequency and pass the fundamental frequency, grounded star and delta transformer are used on both sides of the transmission line. The detailed operating principle of APFC is well-documented in [6]. For the steady-state analysis, the hybrid approach-based model developed in [6] is used. It has been assumed that the amount of active power generated at the fundamental frequency by the series converter is equal to the amount of active power consumed by the series converter at the third-harmonic frequency. The equivalent circuit of the APFC is shown in Fig. 4, where $\bar{V}_p$, $\bar{V}_q$ and $\bar{V}_k$ are the bus voltages of their respective nodes. $\bar{V}_{\mathrm{T}}$, $\bar{V}_{\mathrm{SH}}$, $\bar{V}_{\mathrm{SE1}}$ and $\bar{V}_{\mathrm{SE2}}$ are the voltages injected by SEN transformer, shunt converter, series converter 1 and series converter 2, respectively. $\bar{I}_{\mathrm{T}}$, $\bar{I}_{\mathrm{SH}}$ and $\bar{I}_{pq}$ are the currents injected by the SEN transformer, shunt converter and series line current, respectively. $\bar{Y}_{\mathrm{SH}}$ is the coupling shunt transformer leakage admittance. $R_{\mathrm{C1}}^{\mathrm{SEeq}}$, $R_{\mathrm{C2}}^{\mathrm{SEeq}}$ and $R_{\mathrm{C}}^{\mathrm{SHeq}}$ are the equivalent effective resistances to account switching losses. $\bar{Z}_{pq}^{\mathrm{Eff}}$ is the summation of leakage impedance of series coupling transformer of SEN transformer, the series converter 1, series converter 2 and line impedance between the buses p and q. The detailed modelling procedure is presented in [6].

Fig. 1 *Two-bus system*

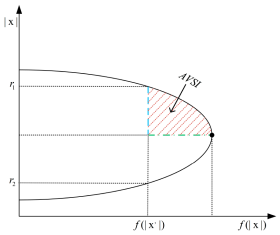

Fig. 2 *Graphical representation of AVSI*

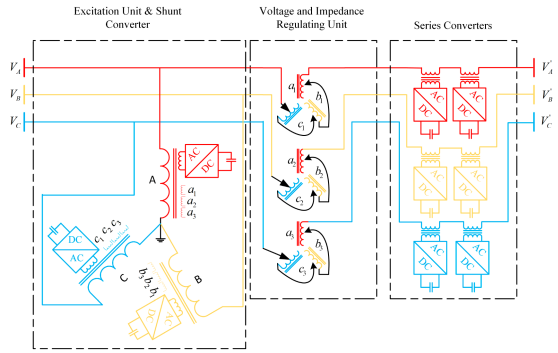

Fig. 3 *Systematic APFC circuit configuration [6]*

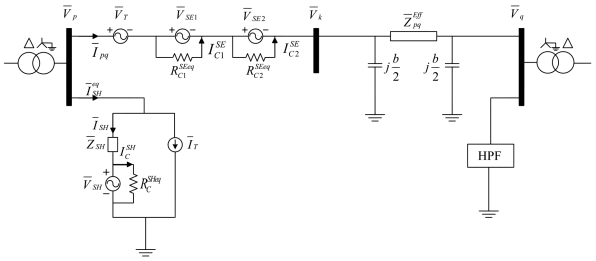

Fig. 4 *APFC equivalent circuit at fundamental frequency [6]*

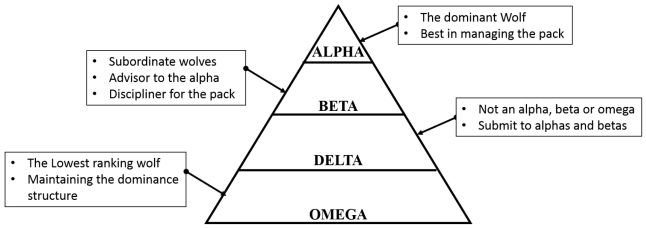

Fig. 5 *Social hierarchy structure of the GWO algorithm*

4 MO problem formulation

In this section, an MO problem for optimal parameter setting of APFC with three equally important objectives is formulated. The considered objective, constraints and fuzzy membership functions are discussed in the following sections.

4.1 Objective functions

In practise, during the planning and operation of power system, more than one objective is required to be achieved. Therefore, the following three objectives are considered:

(i) *Minimisation of power losses:* Traditionally, reactive power loss minimisation is desired not only to increase voltage stability margin but also for economic reasons. Simultaneously, it is desirable to deliver power at minimum active power losses. Therefore, the sum of active and reactive power losses is considered as one of the objectives, which is expresses as follows:

$$\min\ f_1 = P_{\text{loss}} + Q_{\text{loss}} \tag{15}$$

where P_{loss} and Q_{loss} are the total active and reactive power losses in the system.

(ii) *Minimisation of node voltage deviation:* The node voltage deviation is considered as another objective as the node voltage deviation is the measure of voltage quality of the system nodes and its essential to provide regulated node voltage profile across the system. This objective can be expressed as follows:

$$\min\ f_2 = \sum_{i \in L} |1 - V_i| \tag{16}$$

(iii) *Maximisation of AVSI index:* The minimisation of the second objective is not a sufficient measure to define the security level of the power system. Therefore, to accommodate the voltage collapse security, the maximisation of the proposed AVSI is also considered as an objective function. The higher value of AVSI indicates more voltage stability margin available, i.e. more secure. This objective function can be expressed as

$$\max\ f_3 = \min\ (\text{AVSI}_i);\ i \in L \tag{17}$$

4.2 Constraints

The objective functions presented in (15)–(17) are subjected to the following equality and inequality constraints:

$$\begin{aligned} P_i &= V_i \sum_{k=1}^{N} V_k Y_{ik} \cos(\theta_{ik} + \delta_k - \delta_i);\ \forall i \\ Q_i &= V_i \sum_{k=1}^{N} V_k Y_{ik} \sin(\theta_{ik} + \delta_k - \delta_i);\ \forall i \end{aligned} \tag{18}$$

$$\begin{aligned} &P_{\text{G}}^{\min} \le P_{\text{G}} \le P_{\text{G}}^{\max}, \quad Q_{\text{G}}^{\min} \le Q_{\text{G}} \le Q_{\text{G}}^{\max} \\ &V_i^{\min} \le V_i \le V_i^{\max}, \quad \delta_i^{\min} \le \delta_i \le \delta_i^{\max}, \\ &S_{ik} \le S_{ik}^{\max} \end{aligned} \tag{19}$$

The constraints expressed in (18) represent the bus power balance equality constraints. Equation (19) is the set of inequality constraints, which are power generation capability of generators, node voltage limits, node phase angle limits and mega volt ampere (MVA) limits of transmission lines, respectively.

4.3 MO formulation using fuzzy membership function

In this section, the fuzzy approach is used to convert the MO problem to a single-objective problem. In the fuzzy domain, each objective is linked with a membership function. These membership functions indicate the degree of satisfaction of the objectives [15, 16]. A quarter cosine fuzzy membership function is used to evaluate the membership value of the power losses and AVSI index, as conventional trapezoidal fuzzy membership function may reject moderately fitted objectives. The fuzzy membership functions are expressed as follows:

$$\mu f_1 = \begin{cases} 1; & f_1 \le f_{1,\,\min} \\ \cos\left[\dfrac{\pi}{2} \times \dfrac{(f_1(i) - f_{1,\,\min})}{(f_{1,\,\max} - f_{1,\,\min})}\right]; & f_{1,\,\min} < f_1 < f_{1,\,\max} \\ 0; & f_1 \ge f_{1,\,\max} \end{cases} \tag{20}$$

$$\mu f_3 = \begin{cases} 1; & f_{3,\,\min} \le f_3 \le f_{3,\,\max} \\ \cos\left[\dfrac{\pi}{2} \times \dfrac{(f_3(i) - f_{3,\,\min})}{(f_{3,\,\max} - f_{3,\,\min})}\right]; & f_3 < f_{3,\,\min} \end{cases} \tag{21}$$

The exponential fuzzy membership function is used for the node voltage deviation and it can be expressed as follows:

$$\mu f_2 = \begin{cases} 1; & f_{2,\,\min} \le f_2 \le f_{2,\,\max} \\ \exp[m \times |1 - V_i|]; & f_{2,\,\min} \ge f_2 \ge f_{2,\,\max} \end{cases} \tag{22}$$

where μf_i is the membership function value of the objective f_i, whereas $f_{i,\,\min}$ and $f_{i,\,\max}$ are the lower and upper bounds of the variable of the desired ith objective. Here, m is used to vary the time constant of an exponential curve and considered equal to −10. Multiple-objectives which are conflicting in nature cannot be achieved without compromising between different objectives. To obtain overall fuzzy satisfaction for conflicting objectives 'max-geometric mean' is used. The degree of overall fuzzy satisfaction is defined as follows:

$$\mu F = \frac{1}{1 + (\mu f_1 \times \mu f_2 \times \mu f_3)^{1/3}} \tag{23}$$

The system with a minimum degree of overall fuzzy satisfaction, μF, will give the best compromising results. Therefore, function μF is used as a fitness function for the GWO. Therefore, the formulated optimisation problem can be expressed as

$$\min\ \mu F = \frac{1}{1 + \max\ (\mu f_1 \times \mu f_2 \times \mu f_3)^{1/3}} \tag{24}$$

5 GWO algorithm

GWO algorithm introduced by Mirjalili *et al.* [17] is a population-based metaheuristics algorithm which depends on leadership hierarchy and hunting behaviour of wolves. Social hierarchy structure includes four groups of wolfs depending on their role as shown in Fig. 5. Fig. 6 shows the steps for implementing the GWO algorithm considering hunting process, namely tracking, encircling and attacking prey. Here, the population size n is considered as 50; control parameter a is linearly decreased from 2 to 0; random variables r_1 and r_2 are set in the range of 0 and 1; and a maximum number of iterations used is 200.

6 Simulation results and discussion

The proposed model is implemented on IEEE 30-bus test system to investigate the impact of wind and APFC integration. The total real and reactive power demand of the system is found to be 283.40 MW and 126.20 MVAr, respectively. In this system, two big-sized wind farms, each of 50 MW capacity at buses 10 and 22, have been

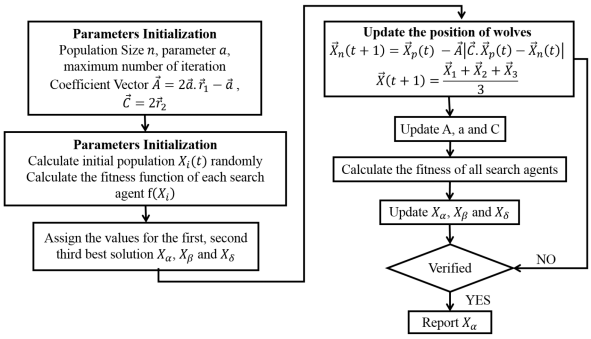

Fig. 6 *Flowchart of the GWO algorithm*

Table 1 Comparison results of IEEE 30-bus test system without APFC in the absence and presence of the wind farms

Loading	Without wind					With wind				
	Value of objectives function				Weakest node (AVSI)	Value of objectives function				Weakest node (AVSI)
	*f*1	*f*2	*f*3	*F*		*f*1	*f*2	*f*3	*F*	
$\lambda = 1$	1	0.964757	1	0.50299	30 (0.594307)	1	0.708136	1	0.528728	30 (0.622483)
$\lambda = 1.25$	0.939297	1	1	0.505218	30 (0.453908)	1	0.96086	1	0.503327	30 (0.482777)
$\lambda = 1.57$	0	0.0883	0.554322	1	30 (0.030687)	0.933638	0.939487	0.990888	0.511685	30 (0.349256)

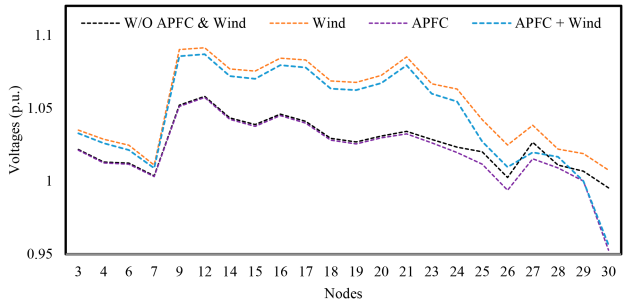

Fig. 7 *Node voltage profile of different cases at* $\lambda = 1$

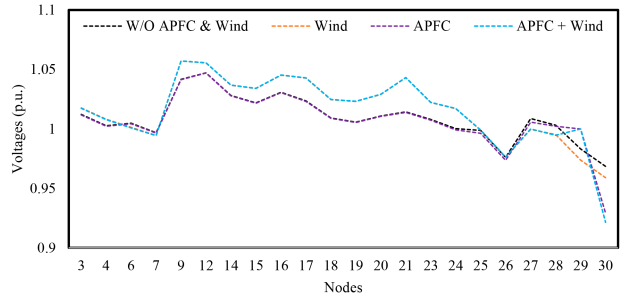

Fig. 8 *Node voltage profile of different cases at* $\lambda = 1.25$

integrated to accommodate high renewable penetration. The problem is formulated in the MATLAB environment and simulated on Intel(R) Core(TM) i3-4150 central processing unit 3.50 GHz processor with 4 GB random access memory. The proposed voltage stability index, i.e. AVSI is used as a measure of voltage stability margin and weakest node in the system. The newly developed FACTS device, i.e. APFC has been considered for optimal parameter setting to minimise the formulated MO problem in the presence and absence of wind farms. The application potential of APFC device has been investigated in the presence and absence of high wind penetration for different loading cases. The following variables are considered as the optimal parameter setting variables:

- The tap (T) setting of SEN transformer of APFC is considered as the first variable to be optimised, and the working range for this variable is [0.01, 1].
- The series voltage source $\left(r_1^{\mathrm{SE}}\right)$ of the SSSC1 of APFC is considered as the second variable to be optimised, and the working range for this variable is $[-0.2, 0.2]$.
- The series voltage source $\left(r_2^{\mathrm{SE}}\right)$ of the SSSC2 of APFC is considered as the third variable to be optimised, and the working range for this variable is $[-0.2, 0.2]$.
- The shunt voltage source (V_{SH}) of the APFC is considered as the fourth variable to be optimised, and the working range for this variable is [0.9, 1.1].

To study the impacts of APFC, the values of AVSI, voltage deviation at the load buses and the sum of both losses are computed for various system conditions using *N–R* method. The results of simulation studies are summarised below.

6.1 Without APFC

At different loading levels in the absence of both APFC and wind farms, the values of different objective functions and weakest node along with AVSI value are presented in Table 1.

Table 1 also presents the results with high wind penetration without APFC. At loading level 1.57, the value of AVSI for node 30 is 0.030687. From Table 1, it can be observed that bus no. 30 has the least value of AVSI in both cases; therefore, the bus 30 has the least voltage stability margin. The voltage stability margin is reducing as the load increases and can be observed from Table 1. Therefore, node 30 is suitable for installation of APFC. The voltage profile of the load buses with and without high wind penetration is shown in Figs. 6–8 at different loading levels. It is observed that in the presence of wind farms, the value of the objective function has significantly decreased from 1 to 0.511685.

6.2 With APFC

The effectiveness of APFC device in the presence and absence of high wind integration for multiple-objectives has been investigated by transforming the MO optimisation problem into a single-objective optimisation problem using the fuzzy logic technique. A quarter cosine and exponential fuzzy membership function are used to find membership values of first and third objectives, and node voltage deviation, respectively. The upper and lower limits of variables of different objectives are shown in Table 2. Table 3 presents the simulation results with APFC in the absence of wind farms. At base case loading, integration of APFC deteriorates the system performance. However, it can be observed that from Tables 1 and 3, APFC enhances the system performance in terms of all objectives at the stressed condition. Also, it improves the AVSI value of node 30 from 0.030687 to 0.9777 at 1.57 loading level. The optimal parameters setting of APFC has been obtained through the proposed fuzzified-GWO algorithm and the obtained values are presented in Table 3.

Table 2 Lower and upper limits of variables of objectives

Objectives	Lower limits, pu	Upper limits, pu
f_1	0.4060	3
f_2	0.95	1.05
f_3	0.4	1

Table 3 Comparison results of IEEE 30-bus test system with APFC in the absence of the wind farms

Loading	Value of objectives function				Optimal parameters setting	AVSI value of node 30
	*f*1	*f*2	*f*3	*F*		
$\lambda = 1$	1	0.9999	1	0.5000	$T = 0.7484$, $r_1^{SE} = 0.1252$, $r_2^{SE} = 0.0051$, $V_{SH} = 0.3323$	0.4594
$\lambda = 1.25$	0.9559	0.9284	0.8359	0.5249	$T = 0.9973$, $r_1^{SE} = 0.0568$, $r_2^{SE} = -0.0037$, $V_{SH} = 0.9001$	0.2729
$\lambda = 1.57$	0.3924	0.1670	0.9991	0.7127	$T = 0.1034$, $r_1^{SE} = -0.1278$, $r_2^{SE} = -0.0120$, $V_{SH} = 0.5869$	0.9777

Table 4 Comparison results of IEEE 30-bus test system with APFC in the presence of the wind farms

Loading	Value of objectives function				Optimal parameters setting	AVSI value of node 30
	f_1	f_2	f_3	*F*		
$\lambda = 1$	0.7141	1	0.9320	0.5339	$T = 0.0997$, $r_1^{SE} = -0.1998$, $r_2^{SE} = -0.1997$, $V_{SH} = 1.0988$	0.3809
$\lambda = 1.25$	0.9118	1	0.8474	0.5215	$T = 0.9956$, $r_1^{SE} = 0.1964$, $r_2^{SE} = -0.1493$, $V_{SH} = 0.9001$	0.2935
$\lambda = 1.57$	0.9406	0.9209	0.7245	0.5388	$T = 0.9962$, $r_1^{SE} = 0.1987$, $r_2^{SE} = -0.0157$, $V_{SH} = 0.9$	0.1928

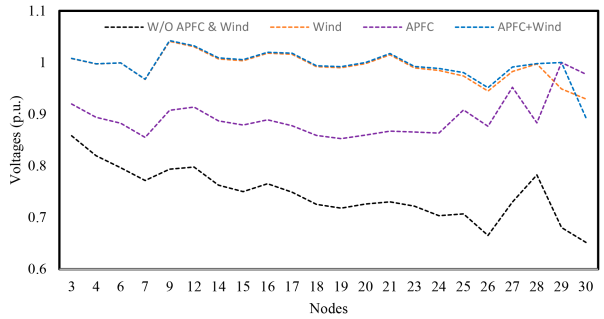

Fig. 9 *Node voltage profile of different cases at* $\lambda = 1.57$

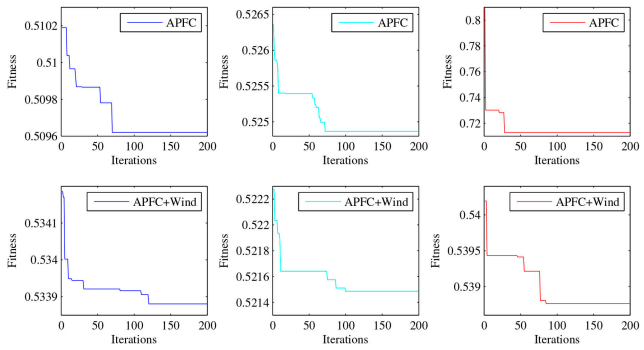

Fig. 10 *Convergence characteristics of GWO for MO minimisation at different loading levels*

The simulation results in the presence of APFC and wind farms are summarised in Table 4. At base case loading, presence of both APFC and wind farms deteriorates the system performance. However, as the system moves toward the high-stressed condition, the APFC and wind farms improve the system performance and it can be observed by comparing Tables 1, 3 and 4. From Tables 3 and 4, it can be observed that in the later case at loading level 1.57, the objective functions f_1 and f_2 are improved by compromising in f_3, to obtain the overall optimal solution. Thereby, a significant reduction in voltage stability margin can be seen from Tables 3 and 4. The node voltage profiles of load buses for different cases are shown in Figs. 7–9 and it is observed that the APFC provides the flexible control over node voltage profile in each case. The convergence curve of GWO in the absence and presence of APFC and wind farms are shown in Fig. 10. The convergence curves at loading levels $\lambda = 1$, 1.25 and 1.57 are denoted by blue, cyan and red colours, respectively, in Fig. 10.

7 Conclusions

In this paper, an optimisation framework has been developed for optimal allocation and parameter tuning of newly developed APFC in order to increase the voltage stability margin of the modern transmission network in the presence and absence of renewables. A new voltage stability index is proposed to determine a node which is more prone to voltage instability, then APFC has been suggested to install. The framework is implemented on the IEEE 30-bus test system for different scenarios and the problem is solved using GWO based on fuzzy logic. The simulation results of different cases are compared. The comparison shows that the proposed approach is found to be promising.

8 References

[1] Kessel, P., Glavitsch, H.: 'Estimating the voltage stability of a power system', *IEEE Trans. Power Deliv.*, 1986, **1**, (3), pp. 346–354

[2] Tiwari, R., Niazi, K.R., Gupta, V.: 'Line collapse proximity index for prediction of voltage collapse in power systems', *Int. J. Electr. Power Energy Syst.*, 2012, **41**, (1), pp. 105–111

[3] Panda, S., Padhy, N.P.: 'Optimal location and controller design of STATCOM for power system stability improvement using PSO', *J. Franklin Inst.*, 2008, **345**, (2), pp. 166–181

[4] Ghahremani, E., Kamwa, I.: 'Optimal placement of multiple-type FACTS devices to maximize power system loadability using a generic graphical user interface', *IEEE Trans. Power Syst.*, 2013, **28**, (2), pp. 764–778

[5] Yorino, N., El-Araby, E.E., Sasaki, H., *et al.*: 'A new formulation for FACTS allocation for security enhancement against voltage collapse', *IEEE Trans. Power Syst.*, 2003, **18**, (1), pp. 3–10

[6] Singh, P., Tiwari, R.: 'Amalgam power flow controller: a novel flexible, reliable and cost effective solution to control power flow', *IEEE Trans. Power Syst.*, 2018, **33**, (3), pp. 2842–2853

[7] Varghese, D., Janamala, V.: 'Optimal location and parameters of GUPFC for transmission loss minimization using PSO algorithm', 2017 Innovations in Power and Advanced Computing Technologies (i-PACT), Vellore, India, 2017, pp. 1–6

[8] Kapetanaki, A., Levi, V., Buhari, M., *et al.*: 'Maximization of wind energy utilization through corrective scheduling and FACTS deployment', *IEEE Trans. Power Syst.*, 2017, **32**, (6), pp. 4764–4773

[9] Sharma, N.K., Ghosh, A., Varma, R.K.: 'A novel placement strategy for FACTS controllers', *IEEE Trans. Power Deliv.*, 2003, **18**, (3), pp. 982–987

[10] Mansour, Y., Xu, W., Alvarado, F., *et al.*: 'SVC placement using critical modes of voltage instability'. IEEE Power Industry Computer Application Conf., Scottsdale, AZ, USA, May 1993, pp. 131–137

[11] Chen, X.R., Pahalawaththa, N.C., Annakkage, U.D., *et al.*: 'Controlled series compensation for improving the stability of multi-machine power systems', *IEE Proc., Gener. Transm. Distrib.*, 1995, **142**, (4), pp. 361–366

[12] Gerbex, S., Cherkaoui, R., Germond, A.J.: 'Optimal location of multi-type FACTS devices in a power system by means of genetic algorithms', *IEEE Trans. Power Syst.*, 2001, **16**, (3), pp. 537–544
[13] Duan, C., Fang, W., Jiang, L.*, et al.*: 'FACTS devices allocation via sparse optimization', *IEEE Trans. Power Syst.*, 2016, **31**, (2), pp. 1308–1319
[14] Ranganathan, S., Kalavathi, S.M.: 'Self-adaptive firefly algorithm based multi-objectives for multi-type FACTS placement', *IET Gener. Transm. Distrib.*, 2016, **10**, (11), pp. 2576–2584
[15] Jang, J.S., Sun, C.T., Mizutani, E.: '*Neuro-fuzzy and soft computing: a computational approach to learning and machine intelligence*' (Prentice-Hall, New Delhi, India, 1997)
[16] Zadeh, L.A.: '*Fuzzy sets, fuzzy logic, and fuzzy systems: selected papers*' (World Scientific, Singapore, 1996), pp. 394–432
[17] Mirjalili, S., Saremi, S., Mirjalili, S.M.*, et al.*: 'Multi-objective Grey Wolf optimizer: a novel algorithm for multi-criterion optimization', *Expert Syst. Appl.*, 2016, **47**, pp. 106–119